A detailed inventory of DNA copy number alterations in four commonly used Hodgkin's lymphoma cell lines

Tom Feys, Bruce Poppe, Katleen De Preter, Nadine Van Roy, Bruno Verhasselt, Pascale De Paepe, Anne De Paepe, Frank Speleman

From the Centre for Medical Genetics (CMGG), Ghent University Hospital Ghent, Belgium (TF, BP, KDP, NVR, ADP, FS); Department of Clinical Chemistry, Microbiology and Immunology; Centre for Molecular Diagnostics, Ghent University Hospital, Ghent, Belgium (BV); Pathological Anatomy, AZ Sint Jan Bruges, Bruges, Belgium (PDP).

Funding: TF is a Ph.D. fellow; BP and BV are Senior Clinicians; and NVR is a Postdoctoral Fellow of the Research Foundation, Flanders (FWO-Vlaanderen). KDP is supported by a grant from the Flemish Institute for the Promotion of Innovation by Science and Technology in Flanders (IWT). This study was supported by the Kinderkankerfonds, the Centrum voor Studie en Behandeling van Gezwelziekten, the FWO-Vlaanderen (grant n. G.0106.05) and GOA (grant n. 12051203). This text presents research results of the Belgian Program of Interuniversity Poles of Attraction initiated by the Belgian State, Prime Minister's Office, Science Policy Programming. The scientific responsibility is assumed by the authors.

Manuscript received November 22, 2006.
Manuscript accepted May 7, 2007.

Correspondence:
Frank Speleman, Centre for Medical Genetics, Ghent University Hospital, De Pintelaan 185, 9000 Ghent, Belgium.
E-mail: franki.speleman@ugent.be

ABSTRACT

Background and Objectives

Classical Hodgkin's lymphoma (cHL) is a common malignant lymphoma characterized by the presence of large, usually multinucleated malignant Hodgkin and Reed Sternberg (HRS) cells which are thought to be derived from germinal center B-cells. In cHL, the HRS cells constitute less than 1% of the tumor volume; consequently the profile of genetic aberrations in cHL is still poorly understood.

Design and Methods

In this study, we subjected four commonly used cHL cell lines to array comparative genomic hybridization (aCGH) in order to delineate known chromosomal aberrations in more detail and to search for small hitherto undetected genomic imbalances.

Results

The aCGH profiles of the four cell lines tested confirmed the complex patterns of rearrangements previously demonstrated with multicolor fluorescence in situ hybridization and chromosomal CGH (cCGH). Importantly, aCGH allowed a much more accurate delineation of imbalances as compared to previous studies performed at a chromosomal level of resolution. Furthermore, we detected 35 hitherto undetected aberrations including a homozygous deletion of chromosomal region 15q26.2 in the cell line HDLM2 encompasing *RGMA* and *CHD2* and an amplification of the *STAT6* gene in cell line L1236 leading to STAT6 overexpression. Finally, in cell line KM-H2 we found a 2.35 Mb deletion at 16q12.1 putatively defining a small critical region for the recurrent 16q deletion in cHL. This region contains the *CYLD* gene, a known suppressor gene of the NF-κB pathway.

Interpretation and Conclusions

aCGH was performed on four cHL cell lines leading to the improved delineation of known chromosomal imbalances and the detection of 35 hitherto undetected aberrations. More specifically, our results highlight *STAT6* as a potential transcriptional target and identified *RGMA*, *CHD2* and *CYLD* as candidate tumor suppressors in cHL.

Key words: Hodgkin's lymphoma, cell line, array CGH.

Haematologica 2007; 92:913-920

Classical Hodgkin's lymphoma (cHL) is a common lymphoma characterized by the presence of malignant mononuclear Hodgkin and multinuclear Reed-Sternberg cells (HRS cells). These HRS cells harbor clonally rearranged and somatically mutated immunoglobulin genes, indicating that in most cases, they are derived from (post-)germinal center B cells.[1] Only in rare cases do HRS cells originate from T-cell lineage precursors.[2] The HRS cells represent only 1% of the affected lymph node and are surrounded by a reactive population of lymphocytes, plasma cells, eosinophils, histiocytes and stromal cells attracted by cytokines and chemokines which are abundantly produced by the HRS cells.[3] Based on the cellular composition and the histological picture of the tumor, cHL is classified into four subtypes: nodular sclerosis, mixed cellularity, lymphocyte predominant and lymphocyte depleted.

Due to the scarcity of HRS cells and their low proliferative index, karyotyping has been severely hampered. Consequently, in contrast to many other malignancies, the profile of genetic aberrations in cHL is still poorly defined and the mechanisms underlying the malignant transformation of HRS cells are only partially understood. Several observations indicate that defects in transcriptional control play a key role. This hypothesis is illustrated by the fact that constitutional activation of the transcription factor nuclear factor kappa B (NF-κB) is a common feature of HRS cells promoting proliferation and survival.[4] Another hallmark of cHL is the aberrant expression of *c-Jun* (*JUN*) and *JUNB*, two members of the AP1 transcription factor family which have been proven to support proliferation in HRS cells.[5]

Due to technical limitations to analyzing pure primary HRS cell populations, extensive efforts were undertaken to establish cell lines from HRS cells as *in vitro* models.[6] This turned out to be extremely difficult, and in the last 30 years, only a few cell lines could be established from cHL patients. In previous studies these cell lines were analyzed by karyotyping and chromosomal comparative genomic hybridization (cCGH).[7-9] Both of these methods do, however, suffer from a limited resolution of 5 to 10 megabases (Mb). More sensitive detection of copy number alterations could allow more refined mapping of breakpoints and identification of hitherto undetected copy number alterations. The recent use of DNA clones spotted in arrays onto glass slides (array CGH; aCGH) rather than entire chromosomes as reporters for detection of DNA copy number changes drastically improved the resolution.[10] We, therefore, decided to re-examine four commonly used cHL cell lines in order to establish a detailed inventory of the copy number alterations. Given the fact that DNA copy number alterations may have a direct effect on gene transcription levels[11] a detailed characterization of the chromosomal imbalances is of importance for further transcriptome analysis of these cell lines.

Design and Methods

Cell lines and culture

The cHL cell lines used originate from patients with cHL of the nodular sclerosis (HDLM2 and L540) or mixed cellularity subtype (KMH2 and L1236). HDLM2 and L540 are of T-cell origin whereas the two other cell lines are of B-cell origin. The cell lines L1236, L540 and KM-H2 are hypotriploid while HDLM2 has a hypodiploid karyotype. All cell lines were obtained from the German Collection of Microorganisms and Cell Cultures (Braunschweig, Germany). Cell lines were cultured following the provider's instructions. After harvesting, DNA was isolated using the QIAamp DNA Blood Mini kit (Qiagen, Hilden, Germany) according to the manufacturer's instructions.

Chromosomal CGH

Metaphase spreads were prepared from phytohemagglutinin-stimulated lymphocytes from healthy individuals according to standard procedures. Slides were stored in plastic boxes with silica gel at -20°C before use. Control DNA was extracted from peripheral blood cells from a healthy male individual as described elsewhere.[12] Test and reference DNA were random prime labeled with spectrum green or spectrum orange using components of the BioPrime DNA labeling system (Invitrogen, Merelbeke, Belgium). *In situ* hybridization, fluorescence microscopy, and digital image acquisition and processing were done according to du Manoir *et al.*[13] with minor modifications.[14] DAPI images of metaphases were recorded prior to hybridization using a Leitz DM microscope, a high-sensitivity integrated monochrome CCD camera and dedicated software (ISIS, MetaSystems, Altlussheim, Germany). Further processing of these images was done according to Vandesompele *et al.*[15]

Array CGH

Using random prime labeling, 500 ng of cell line and control DNA were labeled with Cy3 and Cy5 (BioPrime Array-CGH Genomic Labeling System, Invitrogen, Merelbeke, Belgium). The labeled fragments were suppressed with 125 µg fluorometric QC Cot-1 DNA (Invitrogen, Merelbeke, Belgium), 50 µg fishsperm DNA, 6.5 µg yeast tRNA, and resuspended in 95.5 µL hybridization buffer at 42°C (50% formamide, 7% dextran sulphate, 0.1% Tween 20, 2x SSC, 10mM Tris pH 7.4, 25 mM EDTA pH 8.0). Reference and test DNA were simultaneously hybridized to in-house produced 1Mb resolution BAC arrays, supplemented with tiling paths for chromosomes 3p, 11q and 17 consisting of 4874 clones spotted in triplicate on CodeLink Activated slides (Amersham Biosciences, Diegem, Belgium) using a TECAN HS400 hybridization station (TECAN, Giesen, The Netherlands). The slides were scanned using a GMS 418 Array Scanner

(MWG, Woburn, USA). The scan images were processed with Imagene software (Biodiscovery, Marina Del Rey, USA) and further analyzed with our in-house developed and freely available software tool arrayCGHbase (*http://medgen.ugent.be/arraycghbase/*).[9] Reporters were excluded from analysis if one of the following criteria was fulfilled: signal to noise ratio <3, standard deviation of the $\log_2$ transformed ratios between replicates >0.2 and only one informative replicate. In addition to manual review of aCGH data for detection of gains and losses, we applied the binary segmentation method described by Olshen *et al.*[17]

Quantitative polyerase chain reaction (PCR)

DNA copy numbers were determined in an iCycler real-time PCR detection system using SYBR Green I as the detection format dye. To account for possible variation related to DNA input amounts or the presence of PCR inhibitors, three reference genes *PLK3*, *GRIP2* and *TAL1* were simultaneously quantified in separate tubes for each cell line.

All primers were designed with Primer Express 2.0 software (Applied Biosystems, Foster City, USA). Primers were tested for specificity, absence of single nucleotide polymorphisms (SNP) and secondary structures using the *in silico* assay evaluation tool from RTPrimerDB. Primer sequences are available in the public RTPrimerDB database (*http://medgen.UGent.be/rtprimerdb/*)[18] gene (RTPrimer DB-ID): *STAT6* (3601), *RGMA* (3602), *PLK3* (3529), *TAL1* (1067), *GRIP2* (3603))

The quantitative PCR reaction mix contained 1x SYBR Green I master mix (Eurogentec, Seraing, Belgium), 250 nM of each forward and reverse primer, 10 nM fluorescein and 10 ng template DNA. Each assay included: a no-template control (triplicate), 10 ng of calibrator human genomic DNA (Roche Applied Science, Basel, Switzerland) (quadruplicate) and 10 ng of each cell line (quadruplicate). Cycling conditions were as follows: 10 min at 95°C, 40 cycles of 15 sec at 95°C and 60 sec at 60°C; a melting curve was generated to check the specificity of the PCR reaction. Quantitative PCR data were analyzed with the freely available qbase software (*http://medgen. ugent.be/qbase*).

Fluorescent in situ hybridization (FISH)

The following probes were used for FISH analysis: RP11-481D18 (15q26), RP11-277D13 (15q15.2), RP11-474D13 (12q13.3), RP11-147B17 (16q12.1), RP11-357N13 (16q12.1). All clones were provided by the Welcome Trust Sanger Institute (Cambridge, UK). Clone DNA isolation, labeling and FISH were performed as previously described[19] using SpectrumOrange-dUTP (Vysis, Downers Grove, USA) and Fluorescein-12dUTP (Roche Diagnostics, Germany) as fluorophores. FISH images were recorded using a Zeiss Axioplan 2 microscope, a high-sensitivity integrated monochrome CCD camera and dedicated software (ISIS, MetaSystems, Germany).

Results

Cytogenetic analysis and chromosomal CGH

In order to validate the authenticity of the cell lines and to avoid false positive new findings by aCGH due to secondary aberrations acquired during cell culture or cell line heterogeneity we performed cCGH and aCGH on the same DNA samples for each cell line.

Interestingly, although few differences were found between cCGH and aCGH profiles when comparing for large (>10Mb) chromosomal imbalances, our CGH results showed some remarkable discrepancies with the cell lines studied by Joos *et al.*[8] and Berglund *et al.*[9] The highest number of differences was found for cell line L1236 in which we detected 20 deletions whereas none was detected by Joos *et al.* However, in a subsequent study by these authors using different software and another normalization strategy, results similar to those in our study were obtained (*Joos, personal communication*). Therefore we trust that our results are valid and truly represent the genomic status of the analyzed cell lines.

Array CGH

Comprehensive genomic profiles of gains, losses and amplifications for the cHL cell lines were generated with aCGH. The aCGH profiles of the four cell lines tested confirmed the complex patterns of rearrangements previously demonstrated with karyotyping, multicolor fluorescence *in situ* hybridization (M-FISH) and cCGH[8, 9]. Overall, 157 imbalances were detected, i.e. 81 losses and 76 gains. Cell line KM-H2 displayed the most complex profile with 57 imbalances, whereas in cell lines HDLM2, L540 and L1236 respectively 31, 28 and 40 imbalances were detected. A complete overview of all imbalances is available as supplemental data.

Due to the hypotriploid state observed in three of the investigated cell lines (L1236, L540, KM-H2), single copy number changes often did not reach the aberration threshold. To obtain a more statistically based interpretation of the aCGH data we applied the circular binary segmentation method which turns noisy intensity measurements into regions of equal copy number[17]. Figure 1 illustrates the usefulness of circular binary segmentation for accurate identification of single copy gains or losses.

Improved breakpoint mapping of known genomic imbalances

The arrays used in this study provide a 1 Mb resolution across the genome. As illustrated in Figure 2 (A and B) this increased resolution as compared to cCGH and yields a much more accurate delineation of chromosomal imbalances.

The 1 Mb BAC array was further supplemented with tiling paths for 3p, 11q and chromosome 17 with an average resolution of 150 kb. The power for delineating genomic breakpoints for regions covered by a tiling path is illustrated

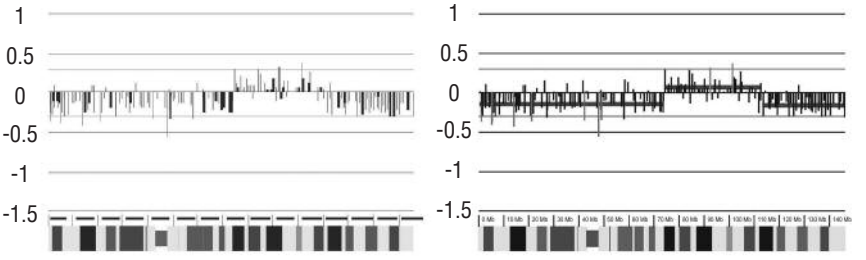

Figure 1. Scoring of chromosomal imbalances through a combination of arrayCGHbase analysis (left) and circular binary segmentation (CBS) (right) illustrated for chromosome 8 in the hypotriploid cell line L540. X-axes: position in Mb along chromosome; Y axes: Log_2 ratio (similar for all aCGH profiles).

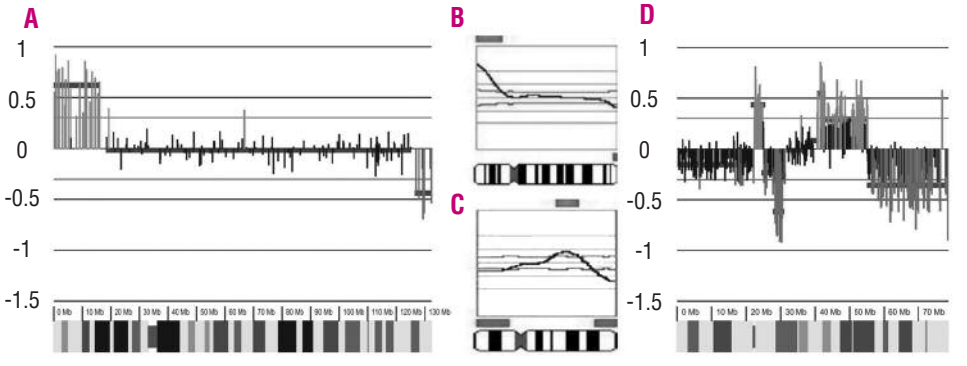

Figure 2. Improved delineation of chromosomal imbalances for chromosome 12 in cell line HDLM2: A. aCGH. B. cCGH. Improved delineation of chromosomal imbalances for chromosome 17 in cell line HDLM2 and detection of additional gain and loss: (C) aCGH, (D) cCGH.

in Figure 2 C and D which shows a comparison between the cCGH and aCGH profiles of chromosome 17 of HDLM2. The aCGH profile clearly allows a much more precise delineation of the chromosomal breakpoints. Moreover, the aCGH profile shows a region of gain and a region of chromosomal loss which were undetected with cCGH.

Previously undetected chromosomal aberrations

In addition to improved breakpoint delineation the present study also resulted in the detection of 35 previously unidentified imbalances. All newly detected aberrations are indicated with an asterix in the overview of all chromosomal imbalances (*Supplemental data*). Figure 3 shows a selection of newly detected imbalances. In addition, a homozygous deletion on the long arm of chromosome 15 (15q26.1) was detected in cell line HDLM2 (Figure 4) in a region which was previously shown to be implicated in a chromosomal rearrangement.[7] The aCGH profile shows a region of hemizygous loss ranging from 15q26.1 to 15qter in which three BAC clones (RP11-237K21, RP11-481D18 and RP11-577O14) are homozygously deleted. The three homozygously deleted BAC span a region of 300 kb (91.2Mb to 91.5 Mb) which harbors only two genes: *RGMA* (repulsive guidance molecule A precursor) and *CHD2* (chromodomain-helicase-DNA-binding protein 2). The presence of the homozygous deletion was confirmed with FISH and quantitative PCR on genomic DNA (Figure 4). In line with these observations quantitative PCR on cDNA of the four cell lines showed the complete absence of *CHD2* expression in cell line HDLM2. Another interesting new finding was a 660 kb wide region of amplification at 12q13.3 in the hypotriploid cell line L1236 (Figure 5). This region is flanked by a region of gain ranging from 12pter to 12q13.3 and a region of loss spanning from 12q14.1 to 12qter and harbors the gene coding for STAT6, a protein that has been reported to be constitutively activated in cHL cell lines and in primary cHL cases. Gain of this locus was independently supported by genomic quantitative PCR analysis and FISH, the latter showing eight copies for the BAC clone spanning the *STAT6* locus. Expression analysis of *STAT6* in the four cell lines showed a two-fold increase in expression in the cell line L1236, in keeping with the observed *STAT6* amplification in this cell line.

The aCGH profile of chromosome 16 in the cell line KM-H2 shows a 16.1 Mb wide region of chromosmal loss ranging from 16q12.1 to 16q21. Within this region we detected an additional deletion of four BAC clones (RP11-305A7, RP11-147B17, RP11-424K7 and RP11-122K22) covering a 2.35 Mb wide region at 16q12.1. This deletion is of interest as this region harbors *CYLD*, a known tumor suppressor gene which inhibits the NFκB pathway, a pathway constitutively activated in cHL. This additional copy number loss for *CYLD* was confirmed with FISH analysis. Quantitative PCR on cDNA of the four cell lines indicated a five-fold decrease of *CYLD* expression in cell line KM-H2 (Figure 6). SNP array data for two of the investigated cell lines (HDLM-2 and L540) are available *http://www.sanger.ac.uk/cgi-bin/genetics/CGP/CGH_home.cgi*.

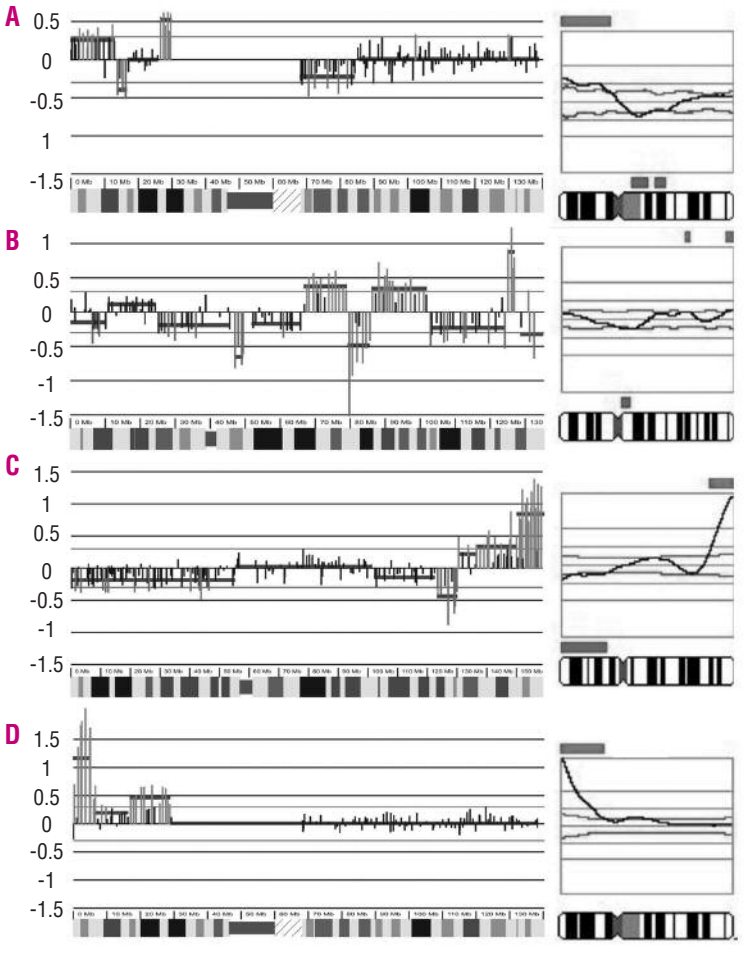

Figure 3. Selection of aCGH results for chromosomal imbalances which remained undetected with cCGH. Left panel: aCGH; right panel: cCGH. A. Undetected partial 9p loss in KM-H2. B. Several undetected gains and losses on chromosome 10 in KM-H2. C. Undetected 7q loss in KM-H2. D. Undetected 9p gain adjacent to amplification in HDLM2.

Discussion

In this study, we subjected four commonly used cHL cell lines to aCGH in order to refine the complex pattern of chromosomal imbalances previously analyzed by low resolution analysis such as karyotyping, M-FISH (HDLM2, L1236 and KM-H2), SKY (L540, HDLM2) and chromosomal CGH (HDLM2, KM-H2, L1236, L540)[6,7,8,9] and to look for small hitherto undetected chromosomal imbalances and homozygous deletions. The present study dramatically improves the delineation of boundaries of known chromosomal gains and losses. Furthermore, 35 new small copy number changes were detected, some of which may be of relevance for our further understanding of HL oncogenesis.

A homozygous deletion at 15q26.2 was detected in the cell line HDLM2. This homozygously deleted region covers only two known genes, *RGMA* and *CHD2*, neither of which has been previously shown to be directly involved in lymphomagenesis. The *RGMA* gene encodes for the repulsive guidance molecule, a protein involved in the guidance of growth cones in developing neurons.[20] Recently *RGMA* was also shown to be expressed in the developing mouse gut.[21] However, no evidence is available for a role of this gene in carcinogenesis. The *CHD2* gene encodes for a chromodomain helicase DNA binding protein. CHD proteins contain a DNA-binding domain as well as a chromodomain motif that can directly affect chromatin structure and gene transcription and therefore CHD proteins are assumed to play an important role in regulating development, cell cycle control and oncogenesis.[22] In line with this it has been suggested that *CHD5* may play a role in the pathogenesis of neuroblastoma.[23] Recently, mutations of the chromodomain helicase DNA-binding protein gene *CHD7* were reported to be the major cause of CHARGE syndrome, a non-random clustering of congenital anomalies including coloboma, heart defects, choanal atresia, retarded growth and development, genital hypoplasia, ear anomalies and deafness.[24] Further investigation is necessary to unveil the potential role of *CHD2* in cHL.

A putative interesting hitherto undetected aberration in cell line L1236 is the amplification of a 660 kb segment including the *STAT6* gene located at 12q13.3. FISH analysis confirmed the presence of eight copies of the clone covering the *STAT6* gene. The signal transducer and activator of transcription (STAT) family of proteins is critical in virtually all cytokine-driven signaling pathways. These proteins are latent in the cytoplasm and become activated through tyrosine phosphorylation which leads to STAT dimerization and translocation to the nucleus, followed by activa-

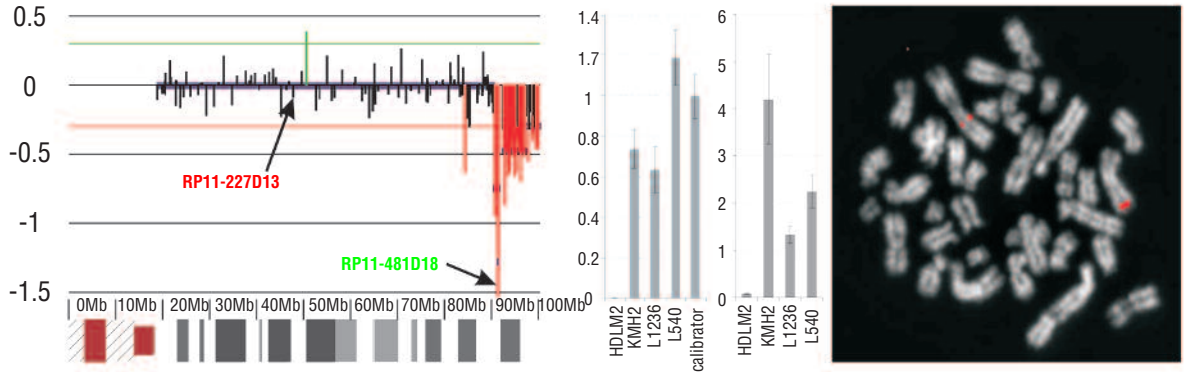

Figure 4. Homozygous deletion at 15q26.1 in HDLM2. Left: aCGH profile for chromosome 15 in HDLM2. Left center bar chart: relative quantities (1: two copies; 0.5: hemizygous loss; 0: homozygous deletion) for the copy number of the *RGMA* gene (located at 15q26.1) determined with quantitative PCR on genomic DNA of the four cell lines and a calibrator. Complete absence of amplification in HDLM2, confirming the homozygous deletion. Right center bar chart: quantitative PCR for *CHD2* gene on cDNA of the four investigated cell lines: complete absence of *CHD2* expression in HDLM2. Right: confirmation of the homozygous deletion with FISH analysis. BAC clones: RP11-481D18 (15q26.1, green, homozygously deleted) and RP11-277D13 (15q15.2, red, two copies).

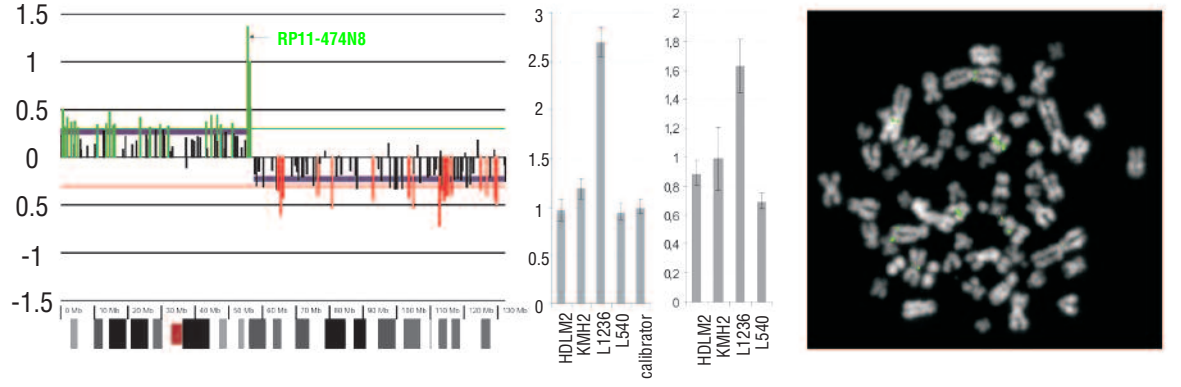

Figure 5. Amplification of the *STAT6* locus at 12q13.3 in the cell line L1236. Left: aCGH profile for chromosome 12 in L1236. Left center bar chart: quantitative PCR for *STAT6* gene on genomic DNA of the four cell lines and a calibrator indicating the presence of five to six copies of *STAT6*. Right center bar chart: expression analysis of *STAT6* in the four cell lines using quantitative PCR: increased *STAT6* expression in L1236. Right: FISH for RP11-474N8 (12q13.3, green, eight copies) confirming the *STAT6* amplification.

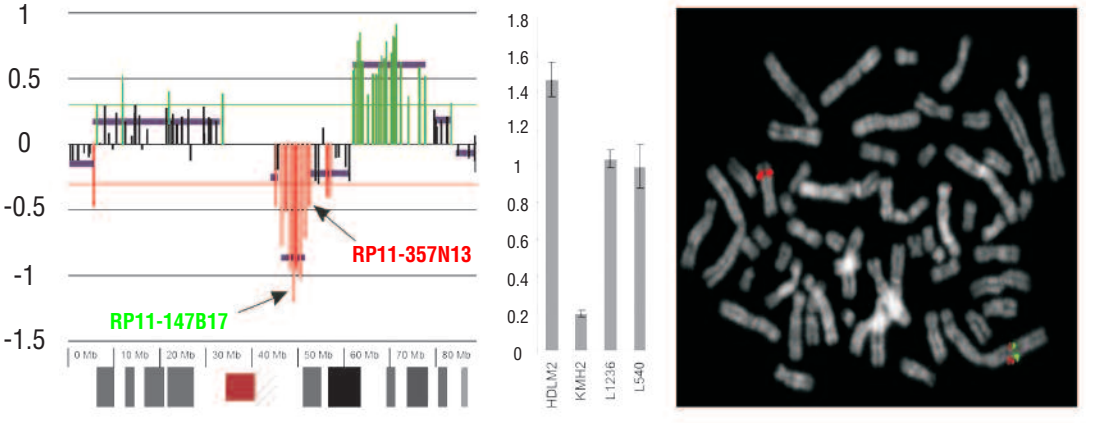

Figure 6. Left: array CGH profile of chromosome 16 in the cell line KM-H2 showing copy loss from 16q12.1 to 16q21 with four clones at 16q12.1 indicating loss of an additional copy. Center: expression analysis of *CYLD* in the four cell lines using quantitative PCR: decreased *CYLD* expression in KM-H2. Right: FISH for RP11-147B17 (green, one copy) and RP11-357N13 (red, two copies) confirming the additional copy loss for RP11-147B17.

tion of transcription.[25] Constitutive activation of STAT3, STAT5 and STAT6 strongly indicates altered JAK/STAT signaling and has been reported for several lymphomas including cHL.[26, 27] Possible mechanisms for this constitutive activation of the JAK/STAT pathway include amplification of the *JAK2* locus [28] and mutations in the *SOCS1* gene,[29] which encodes an inhibitor of kinase activity of JAKs. Skinnider *et al.* proved that STAT6 is constitutively activated in several cHL cell lines, which was shown to be due to autocrine secretion of interleukin-13 in HDLM-2 and L1236 cells.[27] We propose that amplification of the *STAT6* gene may contribute to the constitutive STAT6 activation observed in L1236. This finding is also of interest since several STAT can be targeted by small molecules and hence represent therapeutic targets.

Allelic losses on chromosome 16q have been reported to be frequent in primary HL and have been linked to the loss of E-cadherin expression.[30, 31] In this study we found loss of 16q in two cell lines. In HDLM2 the entire long arm of chromosome 16 is deleted whereas in KM-H2 a 16.1 Mb wide region ranging from 16q12.1 to 16q21 is deleted. The latter region was also reported by Ohshima *et al.* as most commonly deleted in primary HL cases.[30] Remarkably, within this discrete region, a region of 2.35 Mb at 16q12.1 showed loss of an additional copy. Interestingly, this chromosomal region harbors the gene encoding for CYLD, a tumor suppressor gene mutated in familial cylindromatosis, an autosomal-dominant condition that predisposes to multiple skin tumors.[32] CYLD is a deubiquitinating enzyme recently implicated in the modulation of the NF-κB pathway.[33, 34] Upstream of NF-κB, TNF receptor-associated factor 2 (TRAF2) and NEMO (IKKγ), a component of the IKK kinase complex, are conjugated with polyubiquitin chains by the Ubc13/Uev1 ubiquitin-conjugating enzyme complex that catalyzes the formation of a lysine 63 (K63)-linked polyubiquitin chain.[35] Ubiquitination with K48 polyubiquitin chains target proteins for proteosomal degradation. In contrast K63 linked ubiquitin chains usually serve as docking sites for other proteins. The K63 ubiquitination of TRAF2 and NEMO triggers the assembly and activation of the IKK complex leading to NFκB activation.[35] Studies suggest that CYLD can deubiquitinate TRAF2 and NEMO leading to the disassembly of the IKK complex and inhibition of the NF-κB activation.[33, 34]

The present observation of deletion of the CYLD gene is of interest in the light of the known constitutive activation of the NF-κB pathway which has been shown to be a hallmark for cHL. Loss of *CYLD* may therefore constitute a new mechanism underlying NF-κB up-regulation in addition to *REL* gene amplification,[36] ligand-mediated and ligand–independent activation of cell surface receptor CD30,[37] EBV-encoded late membrane protein 1 (LMP1) expression in EBV positive cases[38] or inactivating mutations in the IκBα (*NFKBIA*) or *IκBE* (*NFKBIE*).[39] Further functional studies are required to validate the role of *CYLD* in the pathogenesis of cHL.

In addition to these newly detected small imbalances our study also disclosed a substantial number of larger imbalances, in particular deletions not reported in previous studies.[8,9] One possible explanation for the observed discordances is related to the aCGH software programs and normalization algorithms used for the analysis of these cell lines carrying a high number of imbalances and ploidy changes. In this study we used a ±0.3 threshold which allowed straightforward detection of many copy number changes as well as circular binary segmentation which was helpful in detecting larger (>10 Mb) chromosomal imbalances in near triploid cell lines. Given the importance of cell lines as models for the study of many cancer types, we conclude that aCGH should be performed systematically in order to establish detailed and reliable copy number change profiles.

This genomic information, as illustrated here, can yield information on new critical regions and can be used in combination with gene expression profiling data. However, since the cell lines used in this study were established from patients with advanced stage of disease after several rounds of chemotherapy it is difficult to distinguish between the primary, disease-related and therapy-induced aberrations. Therefore we are currently performing arrayCGH analysis on a series of primary cHL cases. Comparing the chromosomal aberrations detected in these primary cHL cases with the aberrations seen in the cell lines will allow us to identify those chromosomal imbalances specifically implicated in HL-oncogenesis.

In conclusion, aCGH was performed on four cHL cell lines leading to the improved delineation of known chromosomal imbalances and the detection of 35 hitherto undetected aberrations some of which might be interesting in unravelling the molecular events underlying the pathogenesis of cHL. More specifically, our results highlight *STAT6* as a potential transcriptional target and identified *RGMA*, *CHD2* and *CYLD* as candidate tumor suppressors in cHL. These observations encourage genomic and transcriptional analyses of these attractive candidate genes in a clinical setting.

Authors' Contributions

TF: first author; BP: experimental design, critical review of the paper; KDP: CBS data analysis critical review; NVR: FISH data interpretation and critical review of the paper; BV: experimental design, critical review of the paper; PDP: pathology, experimental design, critical review of the paper; ADP: experimental design, critical review of the paper; FS: head of department, experimental design, data analysis, critical review of the paper.

Conflict of Interest

The authors reported no potential conflicts of interest.

References

1. Küppers R, Rajewsky K. The origin of Hodgkin and Reed/Sternberg cells in Hodgkin's disease. Annu Rev Immunol 2002;16: 471-93.
2. Müschen M, Rajewsky K, Bräuninger A, Baur AS, Oudejans JJ, Roers A, et al. Rare occurrence of classical Hodgkin's disease as a T-cell lymphoma. J Exp Med 2000;191: 387-94.
3. Skinnider BF, Mak TW. The role of cytokines in classical Hodgkin lymphoma. Blood 2002; 99: 4283-97.
4. Krappman D, Emmerich F, Kordes U, Scharschmidt E, Dörken B, Scheidereit C. Molecular mechanisms of constitutive NF-KB/Rel activation in Hodgkin/Reed-Sternberg cells. Oncogene 1999;18:943-53.
5. Mathas S, Hinz M, Anagnostopoulos I, Krapmann D, Leitz A, Jundt F, et al. Aberrantly expressed c-Jun and JunB are a hallmark of Hodgkin lymphoma cells, stimulate proliferation and synergize with NF-kB. EMBO 2002;21: 4104-13.
6. Drexler HG. Recent results on the biology of Hodgkin and Reed-Sternberg cells. Leuk Lymphoma 1992; 9:1-25.
7. Macleod RAF, Spitzer D, Bar-Am I, Sylvester JE, Kaufmann M, Wernich A, et al. Karyotypic dissection of Hodgkin's disease cell lines reveals ectopic subtelomeres and ribosomal DNA at sites of multiple jumping translocations and genomic amplification. Leukemia 2000;14:1803-14.
8. Joos S, Granzow M, Holtgreve-Grez H, Siebert R, Harder L, Martin-Subero J, et al. Hodgkin's lymphoma cell lines are characterized by frequent aberrations on chromosomes 2p and 9p including REL and JAK2. Int J Cancer 2003; 103: 489-95.
9. Berglund M, Flordal E, Gullander J, Lui WO, Larsson C, Lagercrantz S, et al. Molecular cytogenetic characterization of four commonly used cell lines derived from Hodgkin lymphoma. Cancer Genet Cytogenet 2003;141:43-8.
10. Solinas-Toldo S, Lampel S, Stilgenbauer S, Nickolenko J, Benner A, Dohner H, et al. Matrix-based comparative genomic hybridization: biochips to screen for genomic imbalances. Genes Chromosomes Cancer 1997;20: 399-407.
11. Tsafrir D, Bacolod M, Selvanayagam Z, Tsafrir I, Shia J, Zeng Z, et al. Relationship of gene expression and chromosomal abnormalities in colorectal cancer. Cancer Res 2006;66:2129-37.
12. Sambrook J, Fritsch EF, Maniatis T. Molecular Cloning: a Laboratory Manual. 2nd edition. Cold Spring Harbor NY: Cold Spring Harbor Laboratory. 1989.
13. du Manoir S, Speicher M, Joos S, Schrock E, Popp S, Dohner H, et al. Detection of complete and partial gains and losses by comparative genomic in situ hybridization. Hum Genet 1993; 90:590-610.
14. Van Roy N, Jauch A, Van Gele M, Laureys G, Versteeg R, De Paepe A, et al. Comparative genomic hybridization analysis of human neuroblastomas: detection of distal 1p deletions and further molecular genetic characterization of neuroblastoma cell lines. Cancer Genet Cyotgenet 1997;92:151-4.
15. Vandesompele J, Van Roy N, Van Gele M, Laureys G, Ambros P, Heimann P, et al. Genetic heterogeneity of neuroblastoma suited by comparative genomic hybridization. Genes Chromosomes Cancer 1998;23:141-52.
16. Menten B, Pattyn F, De Preter K, Robbrecht P, Michels E, Buysse K, et al. ArrayCGHbase: an analysis platform for comparative genomic hybridization microarrays. BMC Bioinformatics 2005;6:124.
17. Olshen AB, Venkatraman ES, Lucito R, Wigler M. Circular binary segmentation for the analysis of array-based DNA copy number data. Biostatistics 2004;5:557-72.
18. Pattyn F, Robbrecht P, De Paepe A, Speleman F, Vandesompele J. RTPrimerDB: the real-time PCR primer and probe database: major update. Nucleic Acid Res 2006;34 (Database issue): D684-8.
19. Van Limbergen H, Poppe B, Michaux L, Herens C, Brown J, Noens L, et al. Identification of cytogenetic subclasses and recurring chromosomal aberrations in AML and MDS with complex karyotypes using M-FISH. Genes Chromosomes Cancer 2002;33:60-72.
20. Matsunaga E, Chétodal E. Repulsive guidance molecule/neogenin: a novel ligand-receptor system playing multiple roles in neural development. Develop Growth Differ 2004;46:481-6.
21. Metzger M, Conrad S, Alvarez-Bolado G, Skutella T, Just L. Gene expression of the repulsive guidance molecules during development of the mouse intestine. Dev Dyn 2005;234:169-75.
22. Woodage T, Basrai MA, Baxevanis AD, Hieter P, Collins FS. Characterization of the CHD family of proteins. Proc Natl Acad Sci USA 1997;94:11472-7.
23. Thompson PM, Gotoh T, Kok M, White PS, Brodeur GM. CHD5, a new member of the chromodomain gene family, is preferentially expressed in the nervous system. Oncogene 2003; 22:1002-11.
24. Vissers LE, Van Ravenswaaij CM, Admiraal R, Hurst JA, De Vries BB, Janssen IM, et al. Mutations in a new member of the chromodomain gene family cause CHARGE syndrome. Nat Genet 2004;36:955-7.
25. Blomberg J, Darnell JE. The role of STATs in transcriptional control and their impact on cellular function. Oncogene 2000;19:2468-73.
26. Kube D, Holtick U, Vockerodt M, Ahmadi T, Haier B, Behrman I, et al. STAT3 is constitutively activated in Hodgkin cell lines. Blood 2001;98:762-70.
27. Skinnider BF, Elia AJ, Gascoyne RD, Patterson B, Trumper L, Kapp, et al. Signal transducer and activator of transcription 6 is frequently activated in Hodgkin and Reed-Sternberg cells of Hodgkin lymphoma. Blood 2002;99: 618-26.
28. Joos S, Küpper M, Ohl S, von Bonin F, Mechtersheimer G, Bentz M, et al. Genomic imbalances including amplification of the tyrosine kinase gene JAK2 in CD30+ Hodgkin cells. Cancer Res 2000;60:549-52.
29. Weniger MA, Melzner I, Menz CK, Wegener S, Bucur AJ, Dorsch K, et al. Mutations of the tumor suppressor gene SOCS-1 in classical Hodgkin lymphoma are frequent and associated with nuclear phosphor-STAT5 accumulation. Oncogene 2006;25:2679-84.
30. Ohshima K, Ishiguro M, Ohgami A, Sugihara M, Seiji H, Suzumiya J, et al. Genetic analysis of sorted Hodgkin and Reed-Sternberg cells using comparative genomic hybridization. Int J Cancer 1999;82:250-5.
31. Ohshima K, Haraoka S, Yoshioka S, Kawasaki C, Tutiya T, Suzumiya J, et al. Chromosome 16q deletion and loss of E-cadherin expression in Hodgkin and Reed-Sternberg cells. Int J Cancer 2001;92:678-82.
32. Bignell GR, Warren W, Seal S, Takahashi M, Rapley E, Barfoot R, et al. Identification of the familial cylindromatosis tumour-suppressor gene. Nat Genet 2000;25:160-5.
33. Kovalenko A, Chable-Bessia C, Cantarella G, Israel A, Wallach D, Courtois G. The tumour suppressor CYLD negatively regulates NF-kB signalling by deubiquitination. Nature 2003;424: 801-5.
34. Trompouki E, Hatzivassiliou E, Tsichritzis T, Farmer H, Ashworth A, Mosialos G. CYLD is a deubiquitinating enzyme that negatively regulates NF-kB activation by TNFR family members. Nature 2003;424:793-6.
35. Zhou H, Wertz I, O'Rourke K, Ultsch M, Seshagiri S, Eby M, et al. Bcl10 activates the NF-kB pathway through ubiquitination of NEMO. Nature 2004; 427:167-71.
36. Joos S, Menz C, Wrobel G, Siebert R, Gesk S, Ohl S, et al. Classical Hodgkin lymphoma is characterized by recurrent copy number gains of the short arm of chromosome 2. Blood 2002;99: 1381-7.
37. Horie R, Watanabe T, Morishita Y, Ito K, Ishida T, Kanegae Y, et al. Ligand-independent signalling by overexpressed CD30 drives NF-kB activation in Hodgkin-Reed-Sternberg cells. Oncogene 2002;21:2493-503.
38. Gires O, Zimber-Strobl U, Gonnella R, Ueffing M, Marschall G, Zeidler R, et al. Latent membrane protein 1 of Ebstein-Barr virus mimics a constitutively active receptor molecule. EMBO 1997;16:6131-40.
39. Jungnickel B, Staratscheck-Jox A, Bräuninger A. Clonal deleterious mutations in the IkBα gene in the malignant cells in Hodgkin's lymphoma. J Exp Med 2000;191:395-401.